https://doi.org/10.31925/farmacia.2023.1.17 **ORIGINAL ARTICLE**

UNEXPECTED BEHAVIOR OF TRISILANOLISOBUTYL-POSS, KEY COMPOUND IN DRUG DELIVERY SYSTEMS, DURING MASS SPECTROMETRY ANALYSIS

CAROLINA COJOCARIU [1,4#], NICULINA DANIELA HĂDADE [2#], MIHAI COSMIN PASCARIU [1,3], CALIN LADASIU [3], ALINA SERB [4]*, EUGEN SISU [4], MARIUS GEORGESCU [5]

[1] *"Vasile Goldiș" Western University of Arad, 86 Liviu Rebreanu Street, 310414, Arad, Romania*
[2] *"Babeş-Bolyai" University, Faculty of Chemistry and Chemical Engineering, Supramolecular Organic and Organometallic Chemistry Centre, 11 Arany Janos Street, 400028, Cluj-Napoca, Romania*
[3] *Renewable Energy and Electrochemistry Department, National Institute of R&D for Electrochemistry and Condensed Matter - INCEMC, 144 Aurel Păunescu-Podeanu Street, 300569, Timișoara, Romania*
[4] *"Victor Babeş" University of Medicine and Pharmacy, Faculty of Medicine, Biochemistry and Pharmacology Department, Biochemistry Discipline, 2 Eftimie Murgu Square, 300041, Timișoara, Romania*
[5] *"Victor Babeş" University of Medicine and Pharmacy, Faculty of Medicine, Function Sciences Department, Physiology Discipline, 2 Eftimie Murgu Square, 300041, Timișoara, Romania*

**corresponding author: aserb@umft.ro*
[#]Authors with equal contribution.

Manuscript received: November 2022

Abstract

The structural investigation of trisilanolisobutyl-POSS, an important precursor for biocompatible materials and drug delivery systems, was performed by (+) ESI-OT-mass spectrometry, using multiple-stage fragmentation. This allowed us to obtain a series of MS^1 - MS^{10} spectra, which are the first to be reported in the field of organosilicon chemistry and pharmaceutical additives. The structure of the fragmentation ions was fully assigned.

Rezumat

Analiza structurală a trisilanolizobutil-POSS, un precursor important pentru materialele biocompatibile și sistemele de eliberare a principiilor active medicamentoase, a fost efectuată prin (+) ESI-OT MS, folosind fragmentarea în etape multiple. Acest lucru ne-a permis să obținem seria de spectre MS^1 - MS^{10}, care sunt pentru prima oară raportate în chimia compușilor organosilicici și a aditivilor farmaceutici. Structura ionilor de fragmentare a fost complet atribuită.

Keywords: trisilanolisobutyl-POSS, ESI-OT-MS, CID, multiple stage fragmentation

Introduction

A drug delivery system (DDS) can be defined as a formulation or material that enables the administration of a therapeutic drug into the body, improving its bioavailability, efficacy and safety [1]. Polyhedral silicon sesquioxanes are a class of nanomaterials that are extremely attractive in the construction of various types of composites [2, 3]. The term silsesquioxanes refers to molecules whose chemical structure can be described by the general formula $R_nSi_nO_{1,5n}$, where R can be hydrogen, alkyl, aryl or other oxyhydrocarbonate or carbonate groups. The molecular architecture of silsesquioxanes can be classified into two categories: (a) cage-like structures, and (b) non-cage-like structures.

Cage-like silsesquioxanes are commonly referred to as polyhedral oligosilsesquioxanes ("POSS") or polyhedral silsesquioxane oligomers [4]. During recent advances in nanomedicine, POSS derivatives have proven their utility, mainly due to their high degree of biocompatibility when used in grafts, advanced DDS, biological sensors, chemotherapy, gene therapy, photodynamic therapy, tissue engineering matrices and cardiovascular implants [1, 5-9].

Mass spectrometry (MS) has been widely used in the characterization of derivatives, oligomers and composites of POSS. For instance, a) one type of composite, obtained by chemical incorporation of monovinyl-POSS into poly(dimethylsiloxane) (PDMS) networks, was investigated by matrix-assisted laser desorption/ionization time-of-flight (MALDI-TOF) mass spectrometry [10], b) the structures of star- and dumbbell-shaped isobutyl-substituted POSS derivatives were confirmed by MALDI-TOF-MS [11], and c) polyurethane functionalized with a pendant furan moiety (FPU) was grafted with polyhedral oligomeric silsesquioxanes (POSS-M), after which the resulting adducts of FPUPOSS-M were analysed by MALDI-TOF-MS [12]. By using the complementary techniques MALDI TOF MS and electrospray-ionisation quadrupole

time-of-flight mass spectrometry (ESI QTOF MS), the following compounds were investigated: a) a co-ordination complex, lithium hepta(ibutyl) silsesquioxane trisilanolate [13]; b) encapsulated fluoride polyhedral oligomeric silsesquioxane (POSS-R) materials, where R = vinyl, phenyl, styrenyl, trifluoropropyl, nona-fluorohexyl [14]; c) a series of polyhedral oligomeric silsesquioxane (POSS) propylmethacrylate (PMA) and styryl oligomers [15]. The structural investigation of trisilanolisobutyl-POSS, using the enhanced features offered by Electrospray-Orbitrap Mass Spectrometry (ESI-OT-MS), which was missing in literature until now, is presented in this paper.

Materials and Methods

1,3,5,7,9,11,14 Heptaisobutyltricyclo [7.3.3.1^{5,11}] heptasiloxane-endo-3,7,14-triol (also named trisilanol-isobutyl-POSS) was purchase from Hybrid Plastic USA, tetrahydrofuran (THF) and methanol (MeOH), chromatographic grades, were from Merck. A POSS stock solution, from which the work solutions were prepared, was obtained by dissolving 8 mg POSS in 1 mL THF (approximately 10^{-2} M). The work solutions were obtained using methanol (1:100 - 1:1000 dilution). The mass spectra were recorded on a Thermo Scientific (LTQ XL Orbitrap) spectrometer, in positive ion mode, using the ESI technique, in the 200 - 2000 *m/z* domain. The following parameters were used: direct infusion of the samples at a flow rate of 5 µL/min, spray voltage, 3 kV; sheath and auxiliary gas flow, 45 and 5 arbitrary units, respectively; capillary temperature, 275°C; capillary voltage, 20 V; and tube lens voltage, +170 V. The number of micro scans was set to three in all experiments. During the Collisions Induces Dissociation (CID) and Higher Energy Collision Dissociation (HCD) fragmentations, isolation of the precursor ions used a 10 *m/z* units windows and the energies indicated in each case.

Results and Discussion

Tandem mass spectrometry has been relatively little illustrated in trisilanolisobutyl-POSS derivatives analysis [16], and ESI-OT-MS capabilities will be exploited in the following POSS investigation. Figure 1 depicts the (+) Electrospray Ionization Orbit Trap High Resolution Mass Spectrometry (ESI-OT-HRMS) spectrum of THF/MeOH solution of trisilanoliso-butyl-POSS. As expected, the MS^1 spectrum shows the typical appearance of a hydroxylated compound [17, 18], with the following ions present: dimer pseudomolecular ions (protonated, monosodium and, respectively, monopotassiated ions), $[2M+H]^+$, $[2M+Na]^+$, as well as $[2M+K]^+$at *m/z* = 1581.5965, 1603.5778 and 1619.5509 respective, along with simple sodium and potassium pseudomolecular ions at *m/z* = 813.2821 and 829.2571. The highest intensity ion is the mono-protonated pseudomolecular ion $[M+ H]^+$ at *m/z* = 791.3019. To certify the assignments of the dimer pseudomolecular ions, the monoprotonated dimer from *m/z* 1581.60 was isolated and then subjected to CID fragmentation, giving the MS^2 spectrum shown in Figure 2.

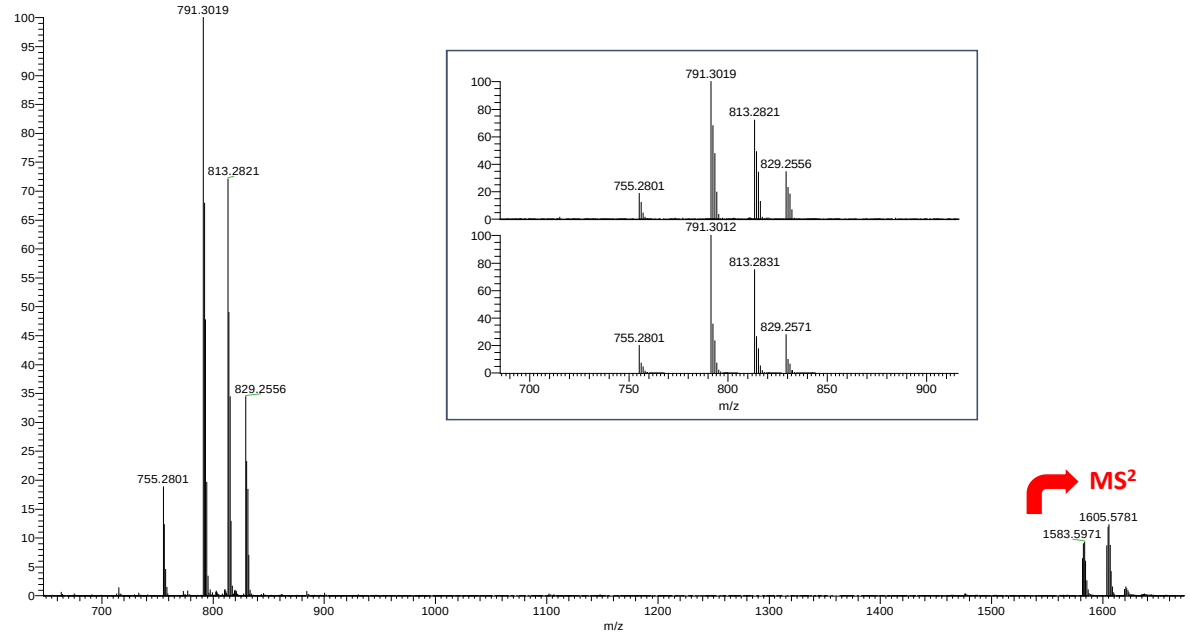

Figure 1.
(+) ESI-OT-HRMS spectrum of Trisilanolisobutyl-POSS ($Si_7O_{12}C_{28}H_{66}$). Insert experimental (top) and calculated (bottom) spectra for $[M+H]^+$, $[M+Na]^+$ and $[M+K]^+$

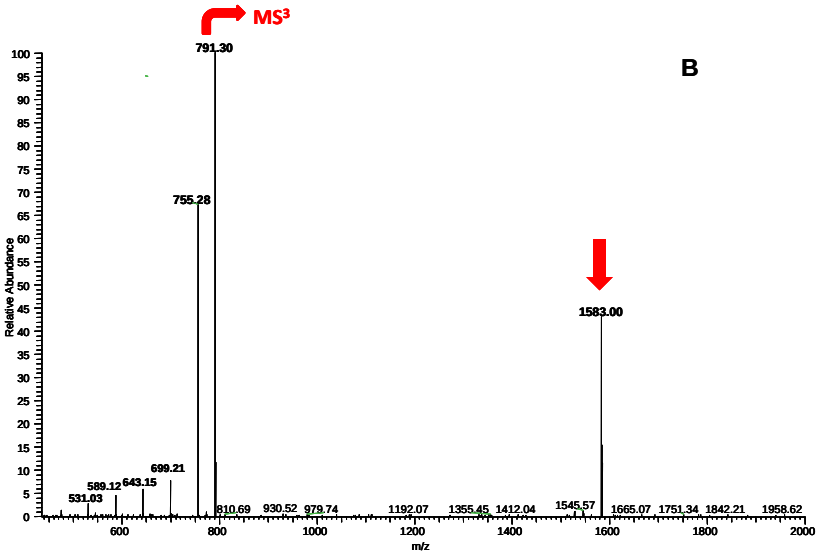

Figure 2.

CID (25 eV) MS^2 of the simple charged ion at *m/z* 1583.00 (the vertical arrow indicates the isolated precursor ion)

The fragmentation pattern suggested by the composition of the fragments from Figure 2 is a strong argument for the fact that the precursor ion isolated and fragmented by CID is the protonated dimer $[2M+H]^+$. Next, the composition of the spectrum suggests that two water molecules are removed from the fragmentation ion with *m/z* 791.30, followed by butene molecules originating from isobutyl radicals which are lost step by step.

Therefore, the ion at *m/z* 791 is further isolated and subjected to HCD fragmentation, giving the MS^3 spectrum (Figure 4, which is shown alongside Figures 5 (MS^4 spectrum), Figure 6 (MS^5 spectrum), Figure 7 (MS^6 spectrum), Figure 8 (MS^7 spectrum), Figure 9 (MS^8 spectrum) and Figure 10 (MS^9 spectrum)).

A significant detail from the MS^3 spectrum, corresponding to the *m/z* 300 - 800 domain, is shown in Figure 3. The analysis of fragmentation ions from the MS^3 spectrum (Figure 3) leads to the following conclusions: a) the fragmentation ions with the highest intensity are those corresponding to the loss of 1 to 5 butene molecules from the doubly dehydrated precursor (*m/z* 699.22; 643.15; 587.09; 531.03; 474.97), b) the fragmentation ions of medium intensity (*m/z* 713.23; 657.17; 615.12; 601.11; 559.06; 545.04; 502.98; 488.98) are those corresponding to the loss of propene molecules, usually accompanied by butene, from the doubly dehydrated precursor (for the generation of propene by McLafferty transposition), and c) fragmentation ions of low intensity correspond to the loss of butyl, water and 0 to 3 butene molecules. Probable mechanism for propene formation by McLafferty transposition from the isobutyl radical is explained in Figure 11 and Figure 12.

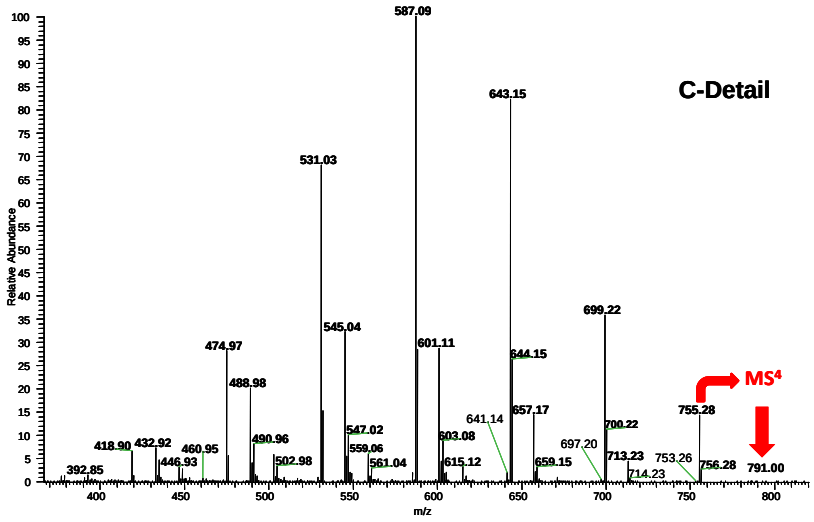

Figure 3.

HCD (45 eV) MS^3 of the simple charged ion at *m/z* 791.00

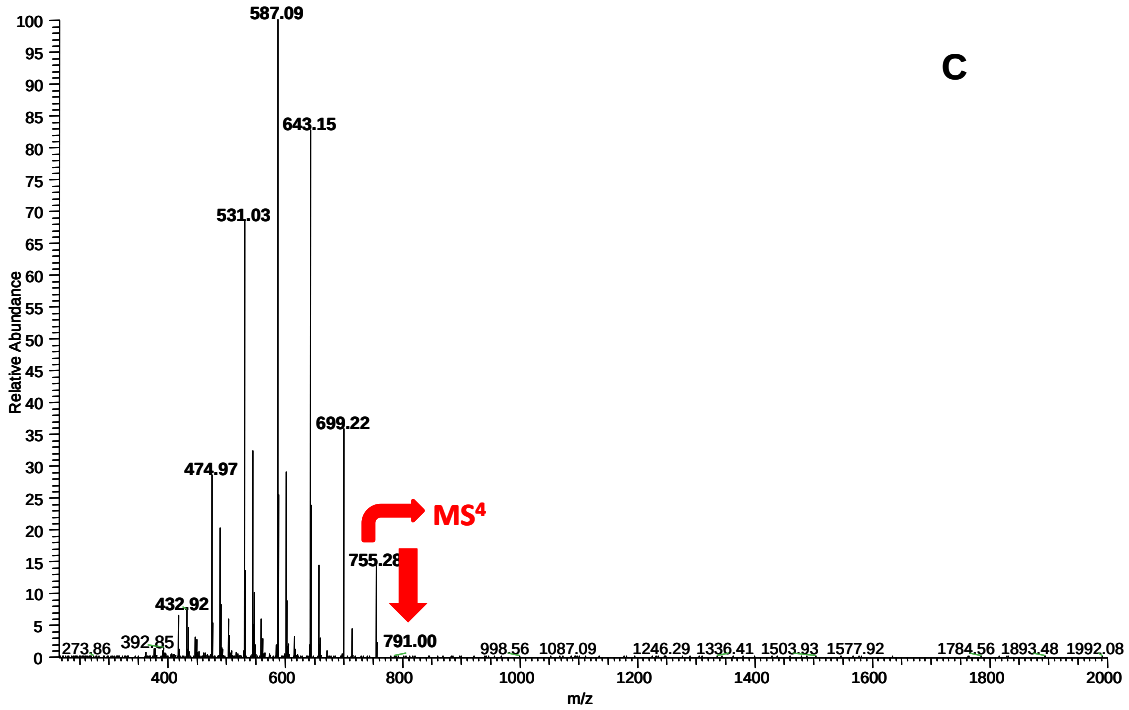

Figure 4.
CID (45 eV) MS^3 of the simple charged ion at *m*/*z* 791.00

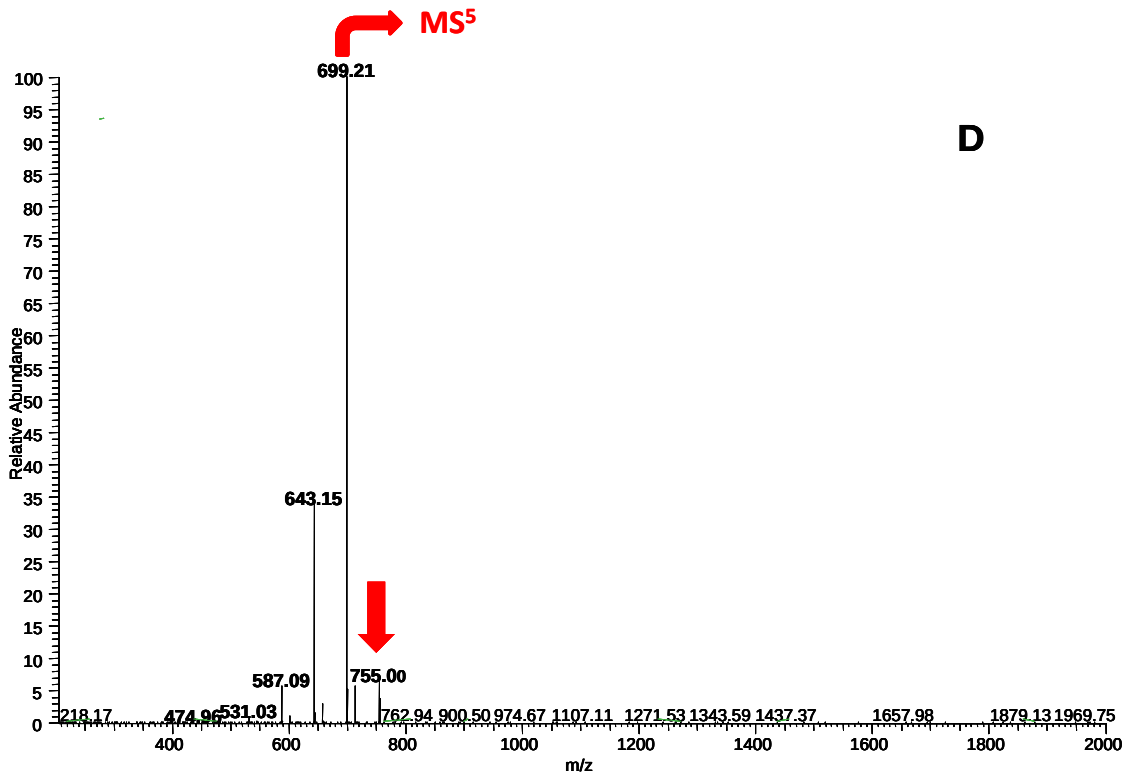

Figure 5.
CID (25 eV) MS^4 of the simple charged ion at *m*/*z* 755.00

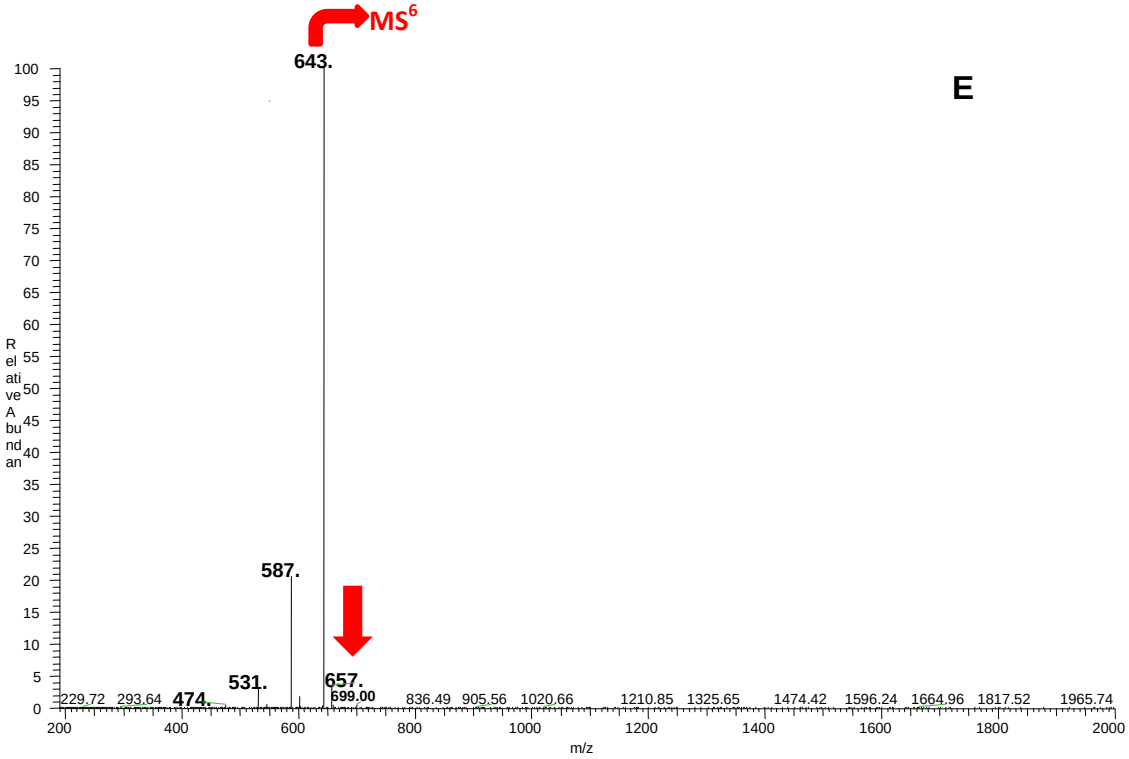

Figure 6.
CID (25 eV) MS^5 of the simple charged ion at *m/z* 699.00

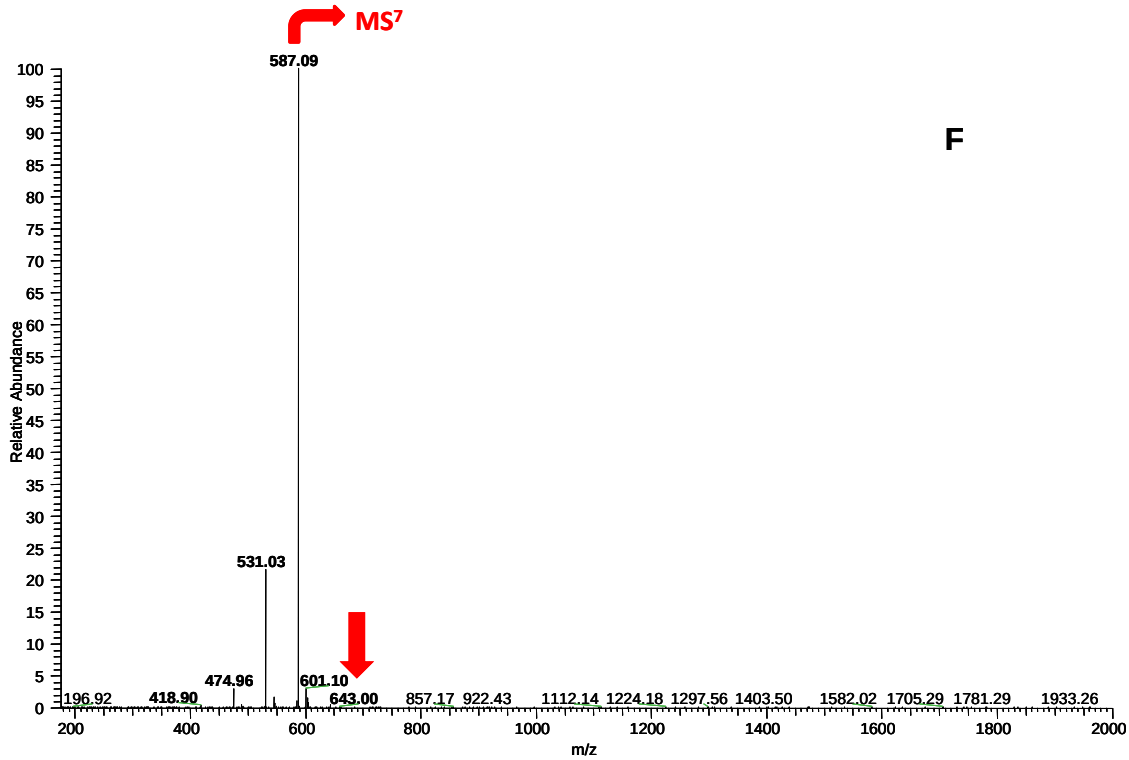

Figure 7.
CID (25 eV) MS^6 of the simple charged ion at *m/z* 643.00

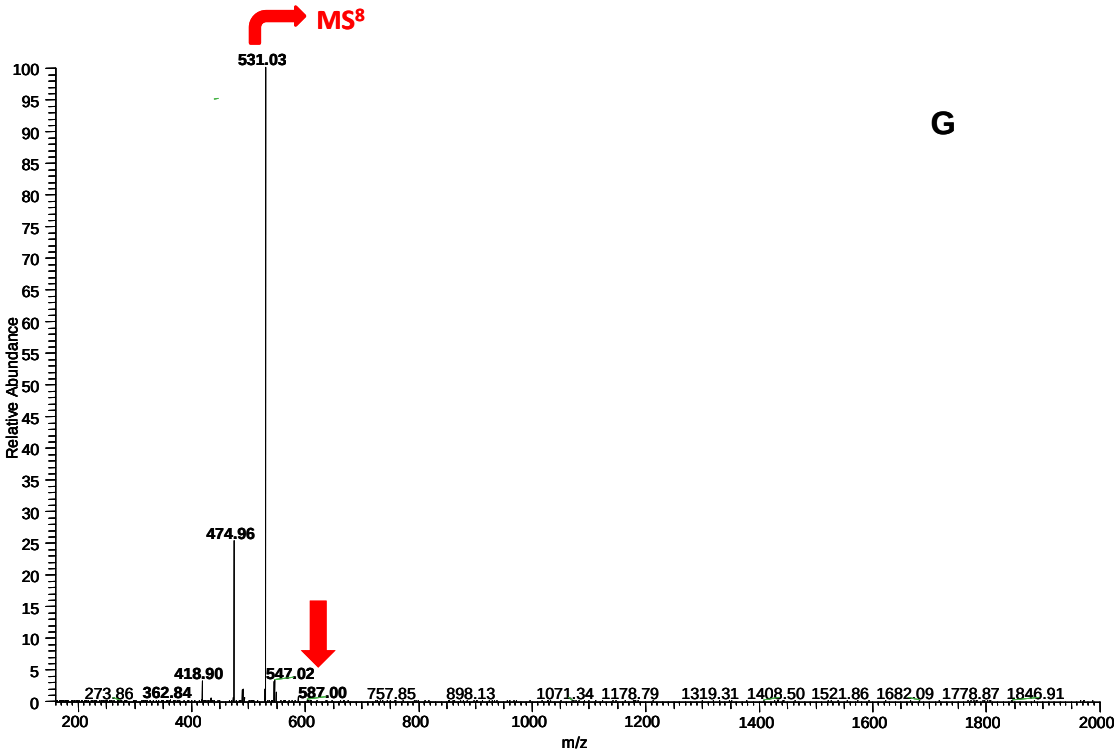

Figure 8.
CID MS^7 of the simple charged ion at *m/z* 587.00

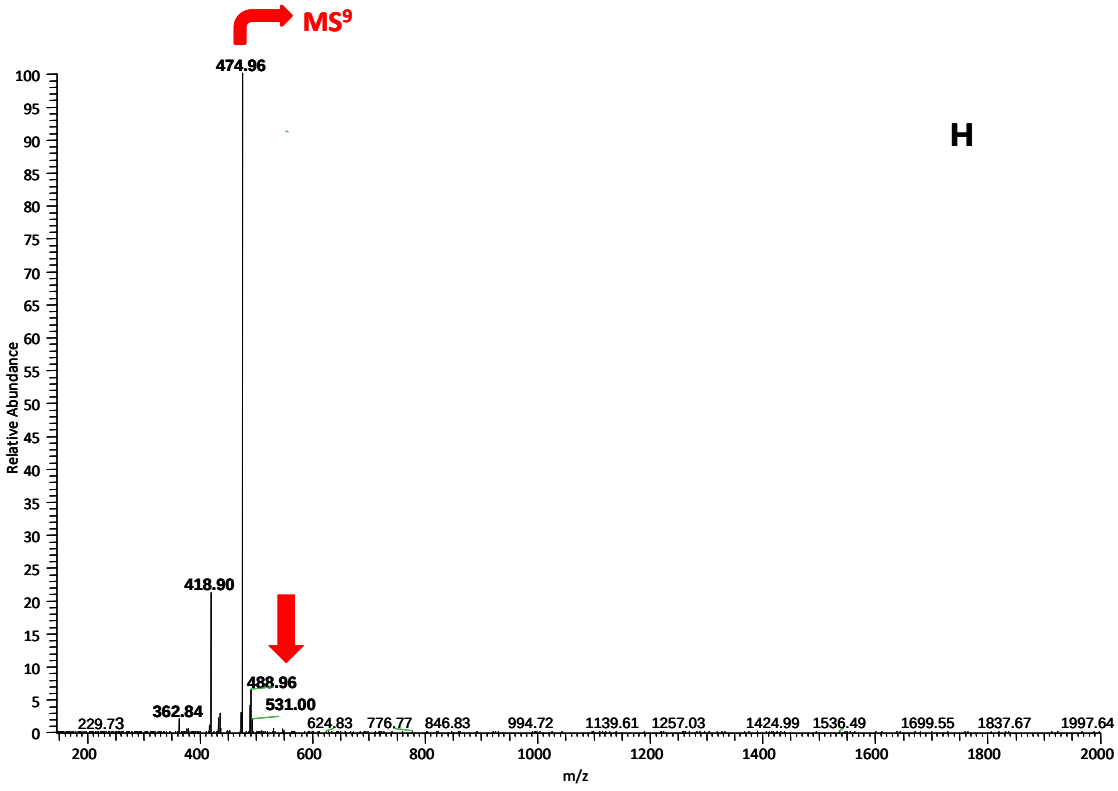

Figure 9.
CID (23 eV) MS^8 of the simple charged ion at *m/z* 531.00

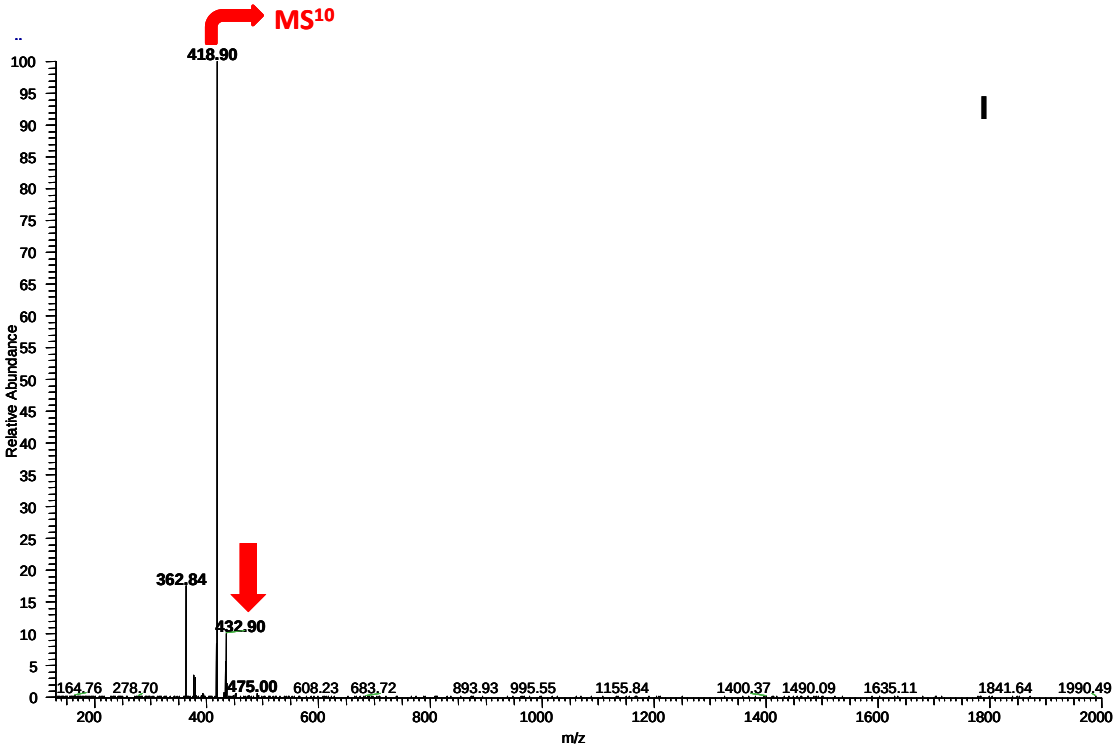

Figure 10.
CID (23 eV) MS^9 of the simple charged ion at *m/z* 475.00

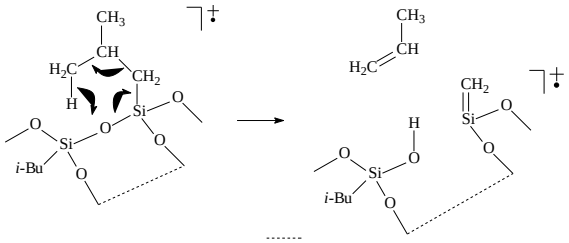

Figure 11.
McLafferty transposition from the isobutyl radical

Elimination of propene causes the formation of a hydroxyl group in the M-42 radical ion. Water and one more molecule of propene can be further cleaved from this ion.

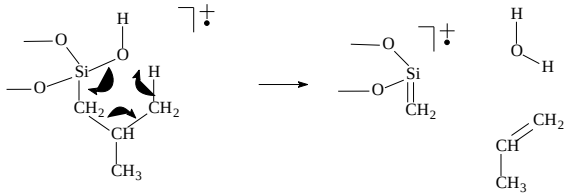

Figure 12.
McLafferty transposition (elimination of water and one molecule of propene)

The *m/z* value assignments observed in MS^4, MS^5, MS^6, MS^7, MS^8 and MS^9 spectra are shown in Table I.

Table I
Assignment of the major ions obtained by CID multistage mass fragmentation and presented in Figures 1A - 1J

No.	*m/z*	Charge	Assignment	Figure	Spectrum
1	1619.55	+1	$[2M + K]^+$	Figure 1	MS^1
2	1603.58	+1	$[2M + Na]^+$	Figure 1	MS^1
3.	1581.60	+1	$[2M + H]^+$	Figure 1	MS^1
4.	829.26	+1	$[M + K]^+$	Figure 1	MS^1
5.	813.28	+1	$[M + Na]^+$	Figure 1	MS^1
6.	791.30	+1	$[M+H]^+$	Figure 1	MS^1
7.	755.28	+1	$[MH - 2H_2O]^+$	Figure 1	MS^1
8	1583.00 #	+1	$[2M + H]^+$	Figure 2	MS^2
9	791.30	+1	$[M+H]^+$	Figure 2	MS^2
10	755.28	+1	$[MH - 2H_2O]^+$	Figure 2	MS^2
11.	699.21	+1	$[MH - 2H_2O\text{-}C_4H_8]^+$	Figure 2	MS^2
12.	643.15	+1	$[MH - 2H_2O\text{-}2C_4H_8]^+$	Figure 2	MS^2
13.	587.09	+1	$[MH - 2H_2O\text{-}3C_4H_8]^+$	Figure 2	MS^2
14.	531.03	+1	$[MH - 2H_2O\text{-}4C_4H_8]^+$	Figure 2	MS^2

No.	*m/z*	Charge	Assignment	Figure	Spectrum
15	791.00 #	+1	$[M+H]^+$	Figure 4	MS^3
16	755.28	+1	$[MH - 2H_2O]^+$	Figure 4	MS^3
17	713.23	+1	$[MH- 2H_2O-C_3H_6]^+$	Figure 4	MS^3
18	699.22	+1	$[MH- 2H_2O-C_4H_8]^+$	Figure 4	MS^3
19	659.15	+1	$[MH- H_2O-2C_4H_9\cdot]^+$	Figure 4	MS^3
20	657.17	+1	$[MH- 2H_2O-C_3H_6-C_4H_8]^+$	Figure 4	MS^3
21	643.15	+1	$[MH - 2H_2O-2C_4H_8]^+$	Figure 4	MS^3
22	615.12	+1	$[MH - 2H_2O-2C_3H_6-C_4H_8]^+$	Figure 4	MS^3
23	603.08	+1	$[MH - H_2O-2C_4H_9\cdot-C_4H_8]^+$	Figure 4	MS^3
24	601.11	+1	$[MH - 2H_2O-C_3H_6-2C_4H_8]^+$	Figure 4	MS^3
25	587.09	+1	$[MH - 2H_2O-3C_4H_8]^+$	Figure 4	MS^3
26	559.06	+1	$[MH - 2H_2O-2C_3H_6-2C_4H_8]^+$	Figure 4	MS^3
27	547.02	+1	$[MH - H_2O-2C_4H_9\cdot-2C_4H_8]^+$	Figure 4	MS^3
28	545.04	+1	$[MH - 2H_2O-C_3H_6-3C_4H_8]^+$	Figure 4	MS^3
29	531.03	+1	$[MH - 2H_2O-4C_4H_8]^+$	Figure 4	MS^3
30	502.98	+1	$[MH - 2H_2O-2C_3H_6-3C_4H_8]^+$	Figure 4	MS^3
31	490.96	+1	$[MH - H_2O-2C_4H_9\cdot-3C_4H_8]^+$	Figure 4	MS^3
32	488.98	+1	$[MH - 2H_2O-C_3H_6-4C_4H_8]^+$	Figure 4	MS^3
33	474.97	+1	$[MH - 2H_2O-5C_4H_8]^+$	Figure 4	MS^3
34	446.93	+1	$[MH - 2H_2O-2C_3H_6-4C_4H_8]^+$	Figure 4	MS^3
35	432.92	+1	$[MH - 2H_2O-C_3H_6-5C_4H_8]^+$	Figure 4	MS^3
36	418.90	+1	$[MH - 2H_2O-6C_4H_8]^+$	Figure 4	MS^3
37	755.00 #	+1	$[MH - 2H_2O]^+$	Figure 5	MS^4
38	713.23	+1	$[MH - 2H_2O-C_3H_6]^+$	Figure 5	MS^4
39	699.21	+1	$[MH - 2H_2O-C_4H_8]^+$	Figure 5	MS^4
40	657.17	+1	$[MH - 2H_2O-C_3H_6-C_4H_8]^+$	Figure 5	MS^4
41	643.15	+1	$[MH - 2H_2O-2C_4H_8]^+$	Figure 5	MS^4
42	601.11	+1	$[MH- 2H_2O-C_3H_6-2C_4H_8]^+$	Figure 5	MS^4
43	587.09	+1	$[MH - 2H_2O-3C_4H_8]^+$	Figure 5	MS^4
44	545.04	+1	$[MH - 2H_2O-C_3H_6-3C_4H_8]^+$	Figure 5	MS^4
45	531.03	+1	$[MH - 2H_2O-4C_4H_8]^+$	Figure 5	MS^4
46	474.96	+1	$[MH - 2H_2O-5C_4H_8]^+$	Figure 5	MS^4
47	699.00 #	+1	$[MH - 2H_2O-C_4H_8]^+$	Figure 6	MS^5
48	657.17	+1	$[MH - 2H_2O-C_3H_6-C_4H_8]^+$	Figure 6	MS^5
49	643.15	+1	$[MH - 2H_2O-2C_4H_8]^+$	Figure 6	MS^5
50	601.10	+1	$[MH - 2H_2O-C_3H_6-2C_4H_8]^+$	Figure 6	MS^5
51	587.09	+1	$[MH - 2H_2O-3C_4H_8]^+$	Figure 6	MS^5
52	545.03	+1	$[MH - 2H_2O-C_3H_6-3C_4H_8]^+$	Figure 6	MS^5
53	531.03	+1	$[MH - 2H_2O-4C_4H_8]^+$	Figure 6	MS^5
54	474.96	+1	$[MH - 2H_2O-5C_4H_8]^+$	Figure 6	MS^5
55	643.00 #	+1	$[MH - 2H_2O-2C_4H_8]^+$	Figure 7	MS^6
56	601.10	+1	$[MH - 2H_2O-C_3H_6-2C_4H_8]^+$	Figure 7	MS^6
57	587.09	+1	$[MH - 2H_2O-3C_4H_8]^+$	Figure 7	MS^6
58	545.03	+1	$[MH - 2H_2O-C_3H_6-3C_4H_8]^+$	Figure 6	MS^6
59	531.03	+1	$[MH - 2H_2O-4C_4H_8]^+$	Figure 7	MS^6
60	490.96	+1	$[MH - H_2O-2C_4H_9\cdot-3C_4H_8]^+$	Figure 7	MS^6
61	474.96	+1	$[MH - 2H_2O-5C_4H_8]^+$	Figure 7	MS^6
62	418.90	+1	$[MH - 2H_2O-6C_4H_8]^+$	Figure 7	MS^6
63	587.00 #	+1	$[MH - 2H_2O-3C_4H_8]^+$	Figure 8	MS^7
64	547.02	+1	$[MH - H_2O-2C_4H_9\cdot-2C_4H_8]^+$	Figure 4	MS^7
65	531.03	+1	$[MH - 2H_2O-4C_4H_8]^+$	Figure 8	MS^7
66	490.95	+1	$[MH - H_2O-2C_4H_9\cdot-3C_4H_8]^+$	Figure 4	MS^7
67	474.96	+1	$[MH - 2H_2O-5C_4H_8]^+$	Figure 8	MS^7
68	418.90	+1	$[MH - 2H_2O-6C_4H_8]^+$	Figure 8	MS^7
69	362.84	+1	$[MH - 2H_2O-7C_4H_8]^+$	Figure 8	MS^7
70	531.00 #	+1	$[MH - 2H_2O-4C_4H_8]^+$	Figure 9	MS^8
71	488.96	+1	$[MH- 2H_2O-4C_4H_8-C_3H_6]^+$	Figure 9	MS^8
72	474.96	+1	$[MH - 2H_2O-5C_4H_8]^+$	Figure 9	MS^8
73	432.92	+1	$[MH - 2H_2O-C_3H_6-5C_4H_8]^+$	Figure 4	MS^8
74	418.90	+1	$[MH - 2H_2O-6C_4H_8]^+$	Figure 9	MS^8

No.	*m/z*	Charge	Assignment	Figure	Spectrum
75	362.84	+1	$[MH - 2H_2O-7C_4H_8]^+$	Figure 9	MS^8
76	475.00 #	+1	$[MH - 2H_2O-5C_4H_8]^+$	Figure 10	MS^9
77	432.90	+1	$[MH - 2H_2O-C_3H_6-5C_4H_8]^+$	Figure 4	MS^9
78	418.90	+1	$[MH - 2H_2O-6C_4H_8]^+$	Figure 10	MS^9
79	362.84	+1	$[MH - 2H_2O-7C_4H_8]^+$	Figure 10	MS^9
80	419.00 #	+1	$[MH - 2H_2O-6C_4H_8]^+$	Figure 13	MS^{10}
81	376.86	+1	$[MH - 2H_2O-C_3H_6-6C_4H_8]^+$	Figure 13	MS^{10}
82	362.84	+1	$[MH - 2H_2O-7C_4H_8]^+$	Figure 13	MS^{10}

denoted precursor ion; MH acronym for $[M+H]^+$

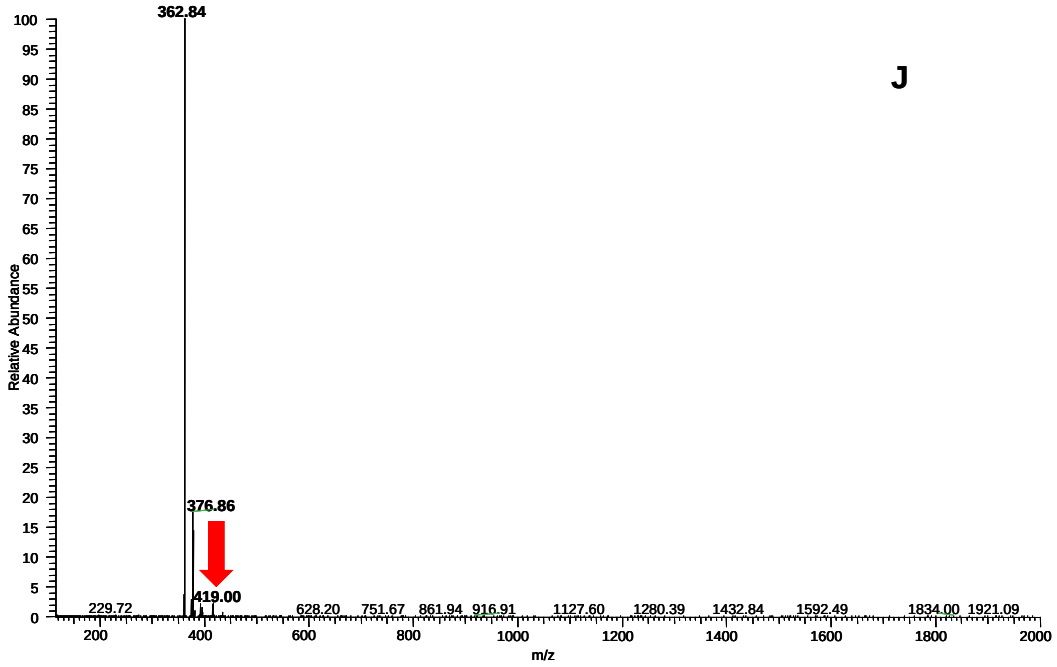

Figure 13.
CID MS^{10} of the simple charged ion at *m/z* 419.00

Figure 13 present the MS^{10} spectrum, which also shows the removal of the last isobutyl residue through isolation and collision-induced fragmentation. So, the "surgical decarbonation" of trisilanolisobutyl-POSS was crowned with success, (Figure 14).

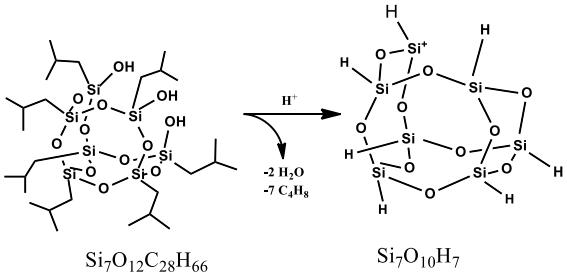

$Si_7O_{12}C_{28}H_{66}$ $Si_7O_{10}H_7$

Figure 14.
(+) ESI-OT-MS "surgery" of Trisilanolisobutyl-POSS

Conclusions

The investigation by (+)ESI-OT-MS, using the multi-stage fragmentation, allowed us to achieve for the first time the performance of MS^1 - MS^{10} analysis for an open-cage silsesquioxanic derivative (a key compound in drug delivery systems) in tandem MS, which is the first reported in the organosilicon chemistry and pharmaceutical additives. The structure of the fragmentation ions has been fully assigned.

Acknowledgement

Part of the research was done at the Centre of Genomic Medicine from the "Victor Babeș" University of Medicine and Pharmacy of Timișoara, Romania, POSCCE 185/48749, contract 677/09.04.2015.

Conflict of interest

The authors declare no conflict of interest.

References

1. Loman-Cortes P, Huq TB, Vivero-Escoto JL, Use of Polyhedral Oligomeric Silsesquioxane (POSS) in Drug Delivery, Photodynamic Therapy and Bioimaging. *Molecules*, 2021; 26(21): 6453.
2. Phillips H, Haddad TS, Tomczak SJ, Developments in nanoscience: polyhedral oligomeric silsesquioxane

(POSS)-polymers. *Curr Opin Solid State Mater Sci.*, 2004; 8(1): 21-29.
3. Ramírez C, Rico M, Torres A, Barral L, López J, Montero B, Epoxy/POSS organic–inorganic hybrids: ATR-FTIR and DSC studies. *Eur Polym J.*, 2008; 44(10): 3035-3045.
4. Wu J, Mather PT, POSS Polymers: Physical Properties and Biomaterials Applications. *Polymer Rev.*, 2009; 49(1): 25-63.
5. Ghanbari H, Cousins BG, Seifalian AM, A Nanocage for Nanomedicine: Polyhedral Oligomeric Silsesquioxane (POSS). *Macromol Rapid Commun.*, 2011; 32(14): 1032-1046.
6. Yahyaei H, Mohseni M, Ghanbari H, Messori M, Synthesis and characterization of polyhedral oligomeric titanized silsesquioxane: A new biocompatible cage like molecule for biomedical application. *Mater Sci Eng C Mater Biol Appl.*, 2016; 61: 293-300.
7. Lukasz J, Mariola M, Janeta M, Szafert S, First step towards a model system of the drug delivery network based on amide-POSS nanocarriers. *RSC Adv.*, 2017; 7: 8394-8401.
8. Neamțu SD, Manda CV, Boldeanu MV, Rotaru I, Neamțu J, Biță A, Croitoru O, Calucică DM, Extraction process assessment and LC-MS analysis of two tyrosine kinase inhibitors in human plasma. *Farmacia*, 2022; 70(5): 855-860.
9. Rezaie J, Akbari A, Functionalization of halloysite nanotubes *via* grafting of polyhedral oligomeric silsesquioxane (POSS) nanoparticles for paclitaxel drug delivery. *Materials Let.*, 2022; 315; 131942.
10. Pan G, Mark JE, Schaefer DW, Synthesis and Characterization of Fillers of Controlled Structure Based on Polyhedral Oligomeric Silsesquioxane Cages and Their Use in Reinforcing Siloxane Elastomers. *J Polym Sci Part B Polym Phys.*, 2003; 41(24): 3314-3323.
11. Araki H, Naka K, Syntheses and properties of star- and dumbbell-shaped POSS derivatives containing isobutyl groups. *Polym J.*, 2012; 44: 340-346.
12. Behera PK, Mondal P, Singha NK, Self-Healable and Ultrahydrophobic Polyurethane-POSS Hybrids by Diels–Alder "Click" Reaction: A New Class of Coating Material. *Macromolecules*, 2018; 51(13): 4770-4781.
13. Prigyai N, Chanmungkalakul S, Ervithayasuporn V, Yodsin N, Jungsuttiwong S, Takeda N, Unno M, Boonmak J, Kiatkamjornwong S, Lithium-Templated Formation of Polyhedral Oligomeric Silsesquioxanes (POSS). *Inorg Chem.*, 2019; 58(22): 15110-15117.
14. Anderson SE, Bodzin DJ, Haddad TS, Boatz JA, Mabry JM, Mitchell C, Bowers MT, Structural Investigation of Encapsulated Fluoride in Polyhedral Oligomeric Silsesquioxane Cages Using Ion Mobility Mass Spectrometry and Molecular Mechanics. *Chem Mater.*, 2008; 20(13): 4299-4309.
15. Anderson SE, Somogyi A, Haddad TS, Coughlin EB, Gadodia G, Marten DF, Ray J, Bowers MT, ESI and MALDI mass spectrometry of large POSS oligomers. *Int J Mass Spectrom.*, 2010; 292(1-3): 38-47.
16. Mao J, Zhang W, Cheng SZD, Wesdemiotis C, Analysis of monodisperse, sequence-defined, and POSS-functionalized polyester copolymers by MALDI tandem mass spectrometry. *Eur J Mass Spectrom.*, 2019; 25(1): 164-174.
17. Bojin LA, Georgescu M, Cojocaru C, Pascariu MC, Purcarea VL, Ivan MV, Puiu M, Dehelean C, Serb AF, Sisu E, Penescu MN, Structural investigation of raw and modified glycans by MALDI-TOF mass spectrometry. *Farmacia*, 2020; 68(5): 891-897.
18. Sisu E, Bosker WTE, Norde W, Slaghek TM, Timmermans JW, Katalinic JP, Cohen-Stuart MA, Zamfir AD, Electrospray ionization quadrupole time-of-flight tandem mass spectrometric analysis of hexamethylenediamine-modified maltodextrin and dextran. *Rapid Commun Mass Spectrom.*, 2006; 20(2): 209-218.